Desalination and Water Treatment
www.deswater.com
doi: 10.1080/19443994.2015.1021842

57 (2016) 8358–8371
April

Taylor & Francis
Taylor & Francis Group

Calix[4]arene-mediated uphill transport of methyl red through bulk liquid membrane: kinetics of operational variables

Fakhar N. Memon, Shahabuddin Memon*, Fozia T. Minhas

National Centre of Excellence in Analytical Chemistry, University of Sindh, Jamshoro 76080, Pakistan, Tel. +92 22 9213429 30; Fax: +92 22 9213431; emails: fakhar_memon2@yahoo.com (F.N. Memon), shahabuddinmemon@yahoo.com (S. Memon), tabasumfouzia@yahoo.com (F.T. Minhas)

Received 12 May 2014; Accepted 3 February 2015

ABSTRACT

The present study demonstrates the successful transport of dyes specially methyl red (MR) using 5,11,17,23-tetra-*tert*-butyl-25,27-dihydroxy-26,28-dimethoxycalix[4]arene (**1**) derivative as a carrier in bulk liquid membrane (BLM). Extraction experiments were performed regarding the optimization of fundamental parameters including pH, decomplexation, dye, and salt concentration. The UV–visible data for stoichiometric ratio suggested 1:1 complexation, which is also verified by Benesi–Hildebrand equation. The high value of formation constant i.e. 8.2×10^4 mol/dm^3 also suggested the strong complexation phenomenon between host and guest molecules. The transport of MR was performed through BLM under optimized conditions such as carrier concentration, type of solvent, and stirrer speed. The kinetic parameters (k_1, k_2, R_m^{max}, t_{max}, J_m^{max}, J_a^{max}) for MR transfer were examined by following kinetic laws of two consecutive irreversible first order reactions. The MR transport was augmented by rise in carrier (**1**) concentration and at high stirring speed. Moreover, the trend of MR transfer in solvents was found to be in the order of $CHCl_3 > CH_2Cl_2 > CCl_4$. Consequently, the developed system was successfully applied on the industrial wastewater samples and **1** was proven as an excellent carrier the removal of dyes through BLM.

Keywords: Bulk liquid membrane; Dyes; Calixarene; Wastewater; Pollution

1. Introduction

The chemistry of dyes is fascinating due to availability of variety of colorful products. However, owing to complex matrix and inability to biodegradation, they are considered as major pollutants of the wastewater running from different industries including textile, plastic, rubber, paper, and cosmetic. It has been reported that about 15% of the dyes are discharged into natural streams during processing and synthesis. Although, industrial wastewater is fairly diluted before disposal but even a little quantity of the dye imparts intense color to water that cause various health hazardous for human and deteriorates the marine life as well [1]. Methyl red (MR) with molecular formula $C_{15}H_{15}N_3O_2$ bearing an azo group is considered as carcinogenic. Student safety sheets for dyes and indicators classify MR as a harmful and irritating dye [2]. Therefore, once the water is contaminated with dye it is very difficult to remove it with traditional methods because some dyes are stable to light. Hence, to solve this problem numerous techniques

*Corresponding author.

have been utilized ranging from physico-chemical to biological treatment [3], including adsorption [4], nanofiltration [5], and oxidation–ozonation [6]. These techniques are certainly employed for the remediation of dye wastewater; however, some of them have tendency to work only at lower concentration and possesses very low degradability with formation of hydroxide sludge.

Since, bulk liquid membrane (BLM) is evolved during past few years as efficient alternatives to all these techniques [7]. Furthermore, the simplicity and facile usage makes BLM widely applicable for the transport of metal ions [8,9], phenols [10], drugs [11], and for the treatment of wastewater [12]. Substantially, carriers of different chemical classes, such as TBAB [13], Cyanex 301 [7], D_2EHPA [14], cationic carrier [15], vegetable oil [16], and Span 80 [17], were employed in liquid membranes (LMs) for the remediation of dyes. Conversely, selective carriers for dyes are still in huge demand.

In this scenario, macrocyclic receptors i.e. cyclodextrins [18] and calixarenes are well reported as promising carriers in LMs [8]. The ordered framework of calixarenes provides a versatile platform for chemical modifications and enables them to act as selective molecular recognizing agents in supramolecular systems [19,20]. In this regard, a number of calixarene derivatives have been frequently applied as carriers through LMs for the transfer of metal ions [8,21] and some basic dyes [22,23]. Recently, our group has evaluated the transport efficiency of calix[6]arene-based carrier in BLM for MR [22]. Thus, to evaluate the cavity size effect the present work demonstrates primarily the extraction efficiency of 5,11,17,23-tetra-*tert*-butyl-25,27-di-hydroxy-26,28-dimethoxycalix[4]arene (**1**) derivative (Fig. 1(a)) for a series of dyes (Fig. 1(b)). Secondly, this derivative has been utilized as a carrier to transport a selective dye MR through BLM. Consequently, the study explores the effect of solvent, stirring rate, and carrier concentration on the transport efficacy.

2. Experimental

2.1. Materials and methods

The preparation of BLM was carried out by utilizing the analytical grade solvents. Deionized water passed from millipore Milli-Q plus water purification system (Elga model classic UVF, UK) was used for the preparation of aqueous solutions. Salts (NaCl, Na_2CO_3, and Na_2SO_4) and dyes (Fig. 1(b)) including methylene blue (MB), methyl green (MG), MR, methyl violate (MV), methyl orange (MO), eosin gelblich (EG), bromocresol green (BCG), bromothymol blue (BTB), and bromophenol blue (BPB) were purchased from Merck supplier. Compound (**1**) was synthesized according to previously reported method [24] and 0.1 M NaOH/HCl solutions were used for pH adjustment.

2.2. Apparatus

UV–visible spectra were recorded on a Perkin Elmer (Shelton, CT 06484, USA) Lambda 35 UV–visible spectrophotometer. For pH adjustment pH meter (781-pH/Ion meter, Metrohm, Herisau, Switzerland) with glass electrode and internal reference electrode was used. To set equal rotation rates of Teflon-coated magnetic bars Gallenkamp magnetic stirrer model APP SS610/5, UK was used. A Gallenkamp thermostat automatic mechanical shaker model BKS 305-101, UK was used for shaking. Transport experiments were performed in U-type cell.

2.3. Liquid/liquid extraction

By following the Pederson procedure [25], 10 mL of 2.5×10^{-5} dye solution was agitated with 10 mL of 1×10^{-3} M carrier **1** (prepared in chloroform) at room temperature. The dye concentration was determined using UV–vis spectrophotometer, the maximum wavelength at which MB, MG, MR, MV, MO and EG, BCG, BTB, BPB absorbs are 663, 629, 430, 586, 463, 515, 420, 432, and 592 nm, respectively. Whereas, extraction percentage was calculated using the following equation,

$$E\% = \left[\frac{(C_0 - C)}{C_0}\right] \times 100 \quad (1)$$

where C_0 and C are the initial and final concentrations of dye in aqueous solution before and after extraction, respectively.

2.4. Complexation study using UV–visible spectroscopy

2.4.1. Jobs plot analysis

The stoichiometric ratio between **1** and MR dye was examined for their inclusion complexation using method of continuous variation (Job's plot). The solutions were prepared by mixing the different ratios (1:9–9:1) of equimolar concentrations (2.5×10^{-5} M) of **1** and MR in CH_2Cl_2. Then, the absorbance was measured at 228 nm.

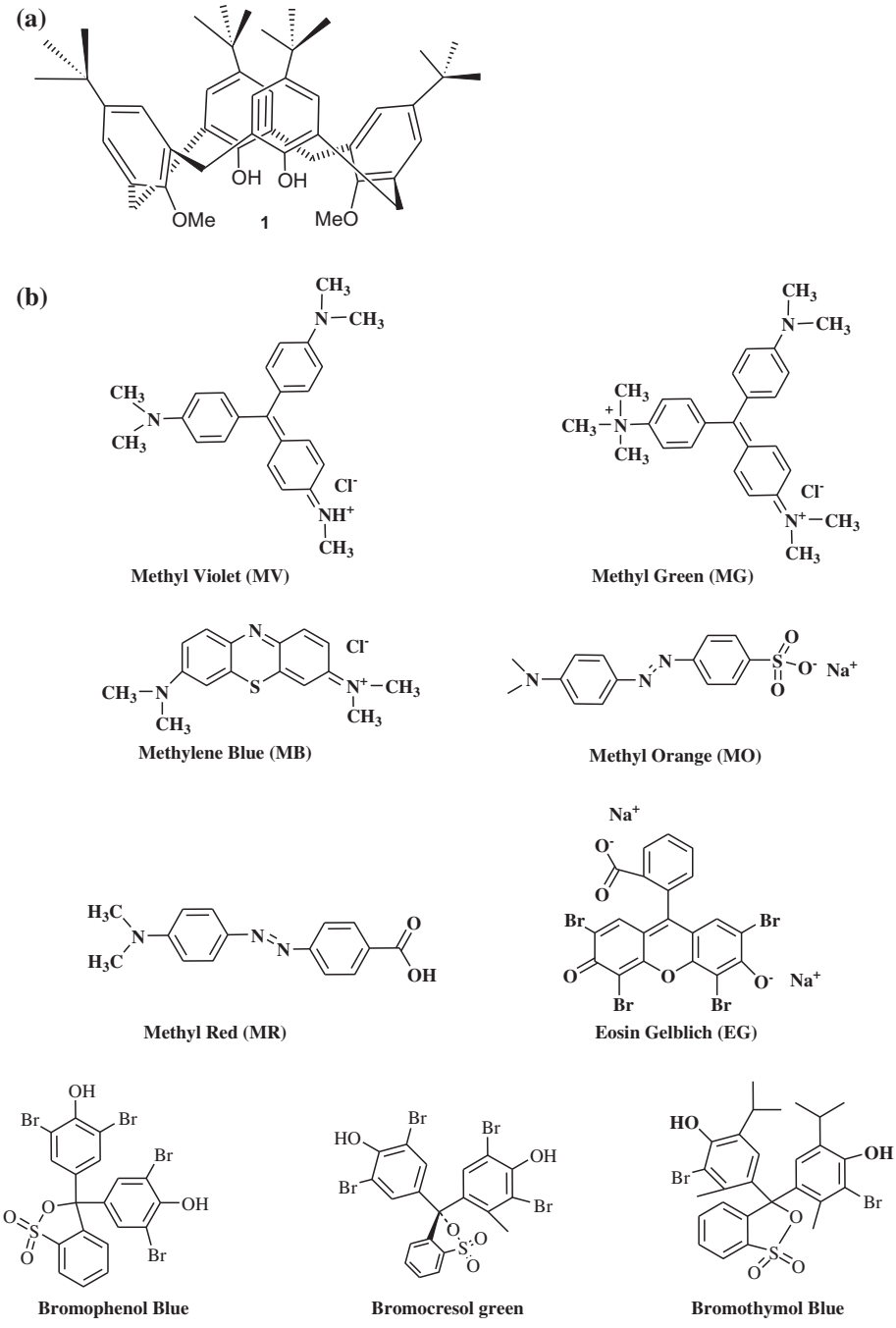

Fig. 1. (a) Chemical structure of 5,11,17,23-tetra-*tert*-butyl-25,27-di-hydroxy-26,28-dimethoxycalix[4]arene (**1**) derivative (carrier **1**) and (b) chemical structures of dyes.

*2.4.2. Calculation of complex formation constant between **1** and MR*

For the spectrophotometric titration, the concentration of **1** was kept constant (1×10^{-5} M) while the concentration of MR was increased continuously from 0.0, 0.2, 0.4, 0.6, 0.8, 1, 2×10^{-5} M. The complex formation constant can be calculated by Benesi–Hildebrand method [26] by using Eq. (2).

$$H + nG \rightarrow H \cdot nG$$

$$\frac{1}{\Delta A} = \frac{1}{K_f \Delta\varepsilon [H][G]^n} + \frac{1}{\Delta\varepsilon [H]} \quad (2)$$

Eq. (2) is valid only for 1:1 complex under the conditions when concentration of donor is smaller than the concentration of acceptor, i.e. [*G*] << [*H*].

Where [*G*] denotes the total concentration of donor, [*H*] refers to the total concentration of acceptor, ε is the molar extinction coefficient of *HG* complex at λ, *n* is the complexation ratio, K_f indicates the formation constant of *HG* complex formation, and ΔA is the change in absorbance of *HG* complex at wavelength λ. The plot of $\frac{1}{\Delta A}$ vs. $\frac{1}{[H][G]}$ yields a straight line. The values of K_f and ε can be calculated from the slope and intercept.

2.5. Liquid/liquid decomplexation

For decomplexation of dye from carrier **1**, the chloroform layer containing carrier and dye was taken and agitated with water at varying pH from 2 to 12 at room temperature. The upper aqueous layer was taken and examined spectrophotometrically. The % decomplexation was calculated using Eq. (3).

$$\%D = \frac{C_3}{C_1} \times 100 \quad (3)$$

where C_1 is the concentration of dye before extraction and C_3 is the concentration of dye released from organic phase.

2.6. BLM experiment

For BLM experiments, the organic phase containing carrier **1** (15 mL) was taken at the bottom of U-type cell followed by careful addition of two aqueous aliquots (10 mL) each separately in donor and receiving compartments. The surface area of the cell at the region of aqueous phases was 2.5 cm^2. The system was stirred at 800 rpm. Initial composition of the components of the cell was:

Donor phase = A dye solution (2.5×10^{-5} M).
Organic phase = Carrier **1** in chloroform (1×10^{-3} M).
Receiving phase = Water at pH 12.

The equal portions of samples from donor and receiving phases were withdrawn simultaneously after some regular time intervals, and the dye concentration was examined spectrophotometrically.

3. Results and discussion

3.1. Liquid–liquid extraction

Primarily, simple liquid–liquid extraction was carried out to evaluate the selectivity of carrier **1** for nine different dyes including MB, MG, MR, MV, MO and EG, BCG, BTB, and BPB. Fig. 2 reveals that the carrier **1** is a good extractant for the transport of MR as compared to other dyes. Furthermore, the uncharged dyes as compared to charged dyes seem to possess better transportation from aqueous phase to organic phase and among all uncharged dyes, carrier **1** is highly

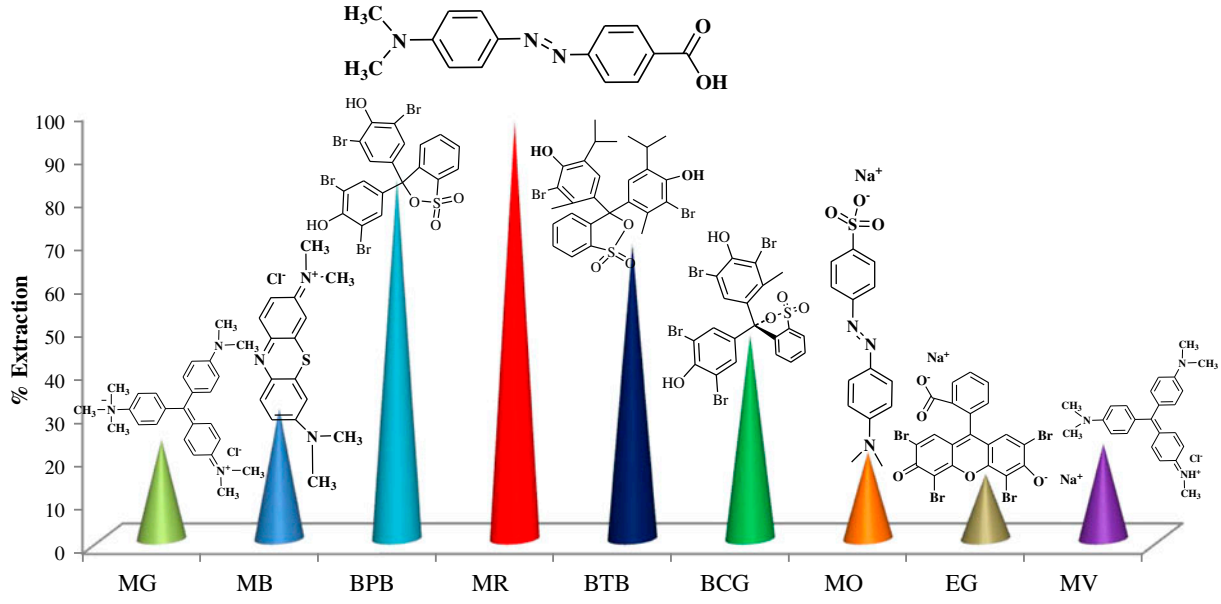

Fig. 2. Comparative extraction efficiency of carrier **1** for various dyes.

selective for MR as compared to other dyes. The effect may be well defined due to the compatibility of the dye molecule with the functionalities of the calixarene moiety. The pronounced interaction may be between the methyl groups (van der Walls forces), carboxylic as well as hydroxyl groups (Hydrogen bonding) of the dye and the carrier **1**.

3.1.1. Effect of pH on receiving phase

In order to enhance and optimize the uptake efficiency of receiving phase for MR, 10 mL solution of carrier **1** in chloroform (1×10^{-3} M) containing MR was agitated with 10 mL of deionized water (receiving phase) whose pH was varied in the range of 2–12 as shown in Fig. 3(a). It can be revealed from Fig. 3(a) that pH 12 is favorable for the back extraction of dye from organic phase containing carrier **1**. The reason behind this decomplexation phenomenon may be that at very basic pH both the dye molecule and the carrier **1** are losing the protons, which are playing a key role in complexation through hydrogen bonding. However, at acidic and neutral pH the protons are intact in complexation phenomenon. Therefore, pH 12 was selected as an optimized pH for the back extraction of MR through BLM.

3.1.2. Effect of salt on the transport of dye

The textile industries utilize many chemical substances during the process of dyeing, printing, desizing, and finishing processes. Therefore, the quality of industrial wastewater is variable and changes with time. Na_2SO_4 (10–20%) is generally added as an electrolyte to the system when some dyes do not provide uniform dye color to the fiber. Similarly, NaCl is utilized during the different processes in the textile and other industries. Therefore, to study the competition effect of electrolytes on the transport of MR, three salts (NaCl, Na_2CO_3, and Na_2SO_4) were used by varying their concentrations ranging from 1 to 50 g/L (Fig. 3(b)). It could be observed from Fig. 3(b) that the extraction efficiency of carrier **1** is not affected with the addition of different concentrations of NaCl and Na_2SO_4. However, the situation was different in case of Na_2CO_3 that being a basic salt alters the pH of solution in donor phase from 5.5 to 11.3 and results a remarkable decrease in the % extraction of MR.

3.1.3. Effect of dye concentration

In order to optimize the concentration of dye, the experiments were carried out by diluting the stock solution of the dye in the range of 1×10^{-4} to

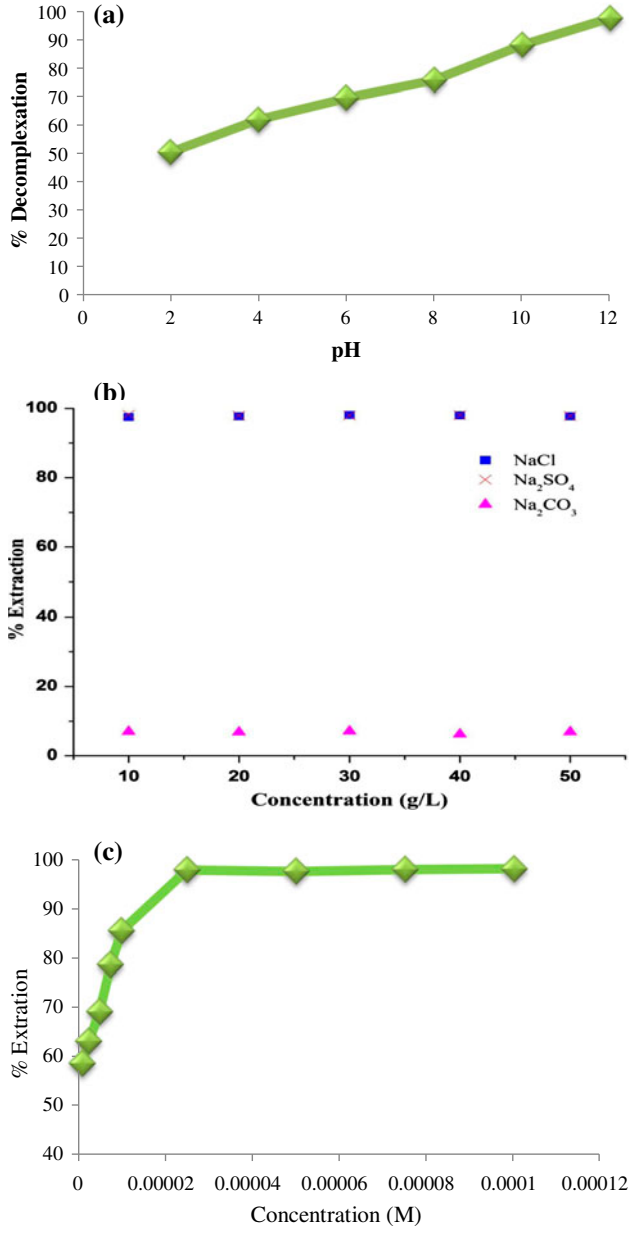

Fig. 3. (a) Effect of pH on decomplexation of MR from carrier (**1**), (b) Effect of salt on % extraction of MR, and (c) Effect of dye concentration on % extraction of MR.

1×10^{-6} M that was agitated with carrier **1** in $CHCl_3$ at room temperature for 30 min. The results are combined in Fig. 3(c). It is quite obvious from Fig. 3(c) that rise in dye concentration successively augments the % extraction of MR. However there is no appreciable change in % extraction of MR beyond 2.5×10^{-5} M dye concentration. Conclusively, the % extraction of MR increases initially with rise in dye concentration because of possible complexation between MR and carrier **1**. Since carrier becomes saturated at

2.5×10^{-5} M dye concentration, therefore additional increase in dye concentration has no effect on % extraction. For this reason, 2.5×10^{-5} M dye concentration is optimized for further study. Moreover, these findings are in league with previously published data [16,27].

3.2. Complexation study

The complexation behavior of **1** with MR was studied in CH_2Cl_2 using UV–visible spectroscopy. Generally, complex formation is associated with the shifting in bands of complexes to shorter or longer wavelengths or at high intensity relative to the free ligand as well as appearance of the new bands. In accordance, the shift in the previous bands and high intensity assures complex making in the present study. It can be revealed from the Fig. 4(a) that the spectra of free ligand **1** show a strong band at 235 nm, which is attributed to the $\pi \rightarrow \pi^*$ and another band at 277–300 nm due to $n \rightarrow \pi^*$ transition. Consequently, addition of guest MR in host (**1**) causes enhancement in the previous bands along with the shift of ~8 nm in the first band i.e. 235–227 nm and ~10 nm shift in another band of **1**. Along with this, the appearance of new band can also be observed at 495 nm as well. These changes in the spectra are clear evidence for the formation of the complex between **1** and MR.

Furthermore, the stoichiometric ratio between **1** and MR complex was calculated using Jobs plot by varying their concentrations (Fig. 4(b)). For **1**-MR complex, the maximum mole fraction value was found to be 0.5, which justifies the 1:1 ratio of the host–guest complex.

In order to evaluate the chromogenic behavior of **1**, the absorption profile as a function of dye concentration was obtained followed by increase in the intensity of absorbance with respect to increased dye concentration (Fig. 4(c)). This profile also confirms the complexation of dye through the binding sites in two lobes of calixarene moiety. Since, the bands at 262–304 nm and 495 nm are significantly affected due to the interaction of dye with methoxy binding sites through van der Waals interactions. While the band at 235 nm, belongs to the aromatic core of the calixarene moiety that has considerably affected confirming endo-complexation.

Furthermore, the insight on 1:1 host–guest complexation between MR (*G*) and **1** (*H*) has also been confirmed by Hildebrand and Benesi plot (Fig. 4(d)) where the calculated values of $\frac{1}{\Delta A}$ and $\frac{1}{[H][G]}$ provide the

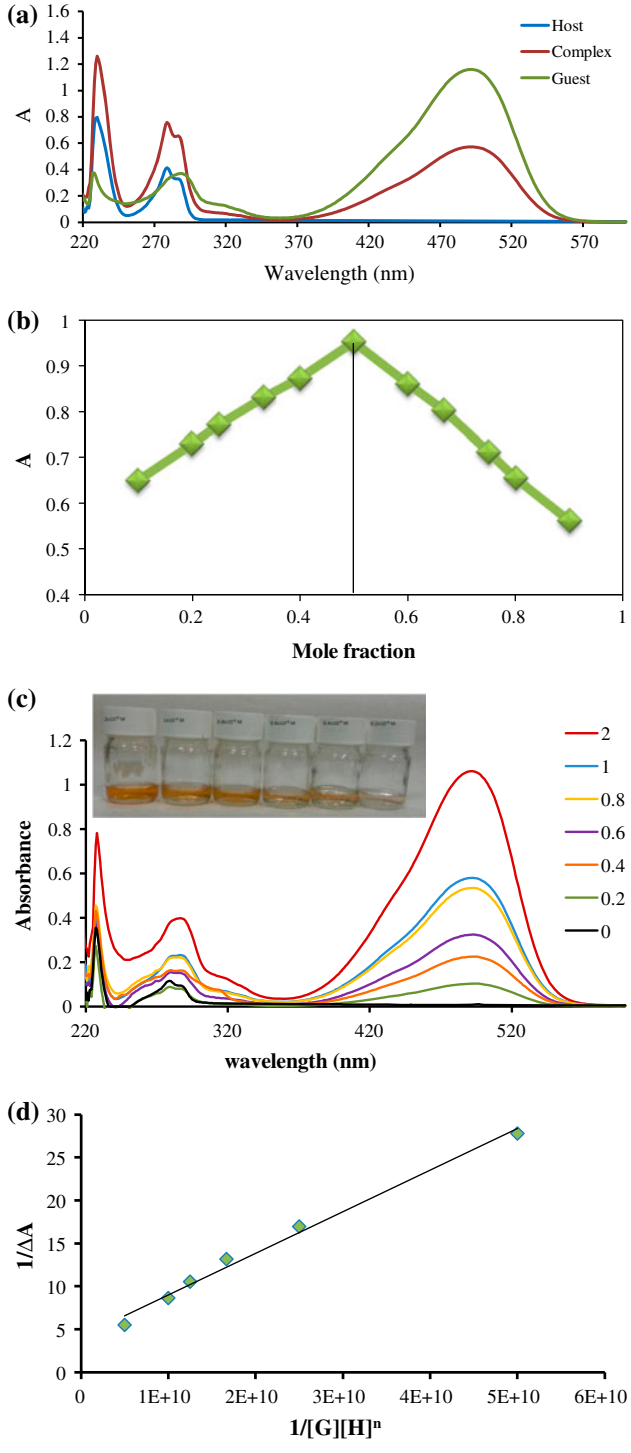

Fig. 4. (a) UV–visible response of **1** (2.5×10^{-5} M) before and after the addition of guest MR, (b) Job's plot of **1** and MR, (c) UV–visible response of **1** (2.5×10^{-5} M) with the various equivalents of MR, and (d) the Benesi–Hildebrand plot of **1**-MR complex.

excellent linear relationship with coefficient of determination $R^2 = 0.99$ having a slope of 5×10^{-10} and intercept 4.133. The value of formation constant ($K_f = 8.2 \times 10^4$ mol dm^{-3}) of **1**-MR complex was calculated from the ratio of slope/intercept.

The higher value of the formation constant suggests the strong complexation between host and guest molecules.

3.3. Bulk liquid membrane

3.3.1. Kinetic procedure

Kinetics for the transport of MR was directly determined in donor and receiving phases using spectrophotometer at regular intervals of 30 min. Consequently, carrier concentration, stirrer speed, and type of solvent were studied in detail through BLM. The subsequent changes in the concentration of dye were determined from the material balance between two phases, i.e.

$$R_d + R_m + R_a = 1 \tag{4}$$

where R_d is dimensionless reduced concentration of dye in donor, R_m in membrane, and R_a in acceptor phase. The values of these parameters are calculated from the following Equation.

$$R_d = \frac{C_d}{C_{do}} \quad R_m = \frac{C_m}{C_{do}} \quad R_a = \frac{C_a}{C_{do}} \tag{5}$$

where C_0 is initial concentration of dye in the donor phase.

The kinetic scheme for consecutive reaction systems can be described by the following rate equations:

$$\frac{dR_d}{dt} = -k_1 R_d \equiv J_d \tag{6}$$

$$\frac{dR_m}{dt} = k_1 R_d - k_2 R_m \tag{7}$$

$$\frac{dR_a}{dt} = k_2 R_m = J_a \tag{8}$$

where J is the flux, when $k_1 \neq k_2$; and integrating the above differential equations gives;

$$R_d = \exp(-k_1 t) \tag{9}$$

$$R_m = \frac{k_1}{k_2 - k_1}[\exp(-k_1 t) - \exp(-k_2 t)] \tag{10}$$

$$R_a = 1 - \frac{k_1}{k_2 - k_1}[k_2 \exp(-k_1 t) - k_1 \exp(-k_2 t)] \tag{11}$$

while the maximum values of R_m and t_{max} (when $dR_m/dt = 0$) can be written as;

$$R_m^{max} = \left(\frac{k_1}{k_2}\right)^{-k_2/(k_1 - k_2)} \tag{12}$$

$$t_{max} = \left(\frac{1}{k_1 - k_2}\right) \ln \frac{k_1}{k_2} \tag{13}$$

combining Eqs. (12) and (13), the following relationship can be obtained.

$$k_2 = \frac{\ln\left(\frac{1}{R_m^{max}}\right)}{t_{max}} \tag{14}$$

Numerical analysis by non-linear curve fitting permits the rate constants to be determined, the value of k_1 is directly obtained by iteration from Eq. (9). This value is introduced as a constant value in Eqs. (10) and (11). An initial value of k_2 is obtained from Eq. (14) and introduced in Eqs. (10) and (11) and iterated.

By considering the first-order time differentiation Eqs. (9)–(11) at t_{max}, one obtains the following equations:

$$\left.\frac{dR_d}{dt}\right|_{max} = -k_1 \left(\frac{k_1}{k_2}\right)^{-k_1/(k_1 - k_2)} \equiv J_d^{max} \tag{15}$$

$$\left.\frac{dR_a}{dt}\right|_{max} = k_2 \left(\frac{k_1}{k_2}\right)^{-k_2/(k_1 - k_2)} \equiv J_a^{max} \tag{16}$$

$$\left.\frac{dR_m}{dt}\right|_{max} = 0 \tag{17}$$

$$-\left.\frac{dR_d}{dt}\right| = \left.\frac{dR_a}{dt}\right| \tag{18}$$

It may be noted that at $t = t_{max}$ the system be in steady state because the concentration of dye in the membrane does not change with time (Eq. (17)). As a result, the exit and entrance fluxes are equal and have opposite signs (Eq. (18)).

It can be seen that R_d vs. t yields a decreasing monoexponential curve, whereas the time variation of both R_m and R_a is biexponential. The actual numerical

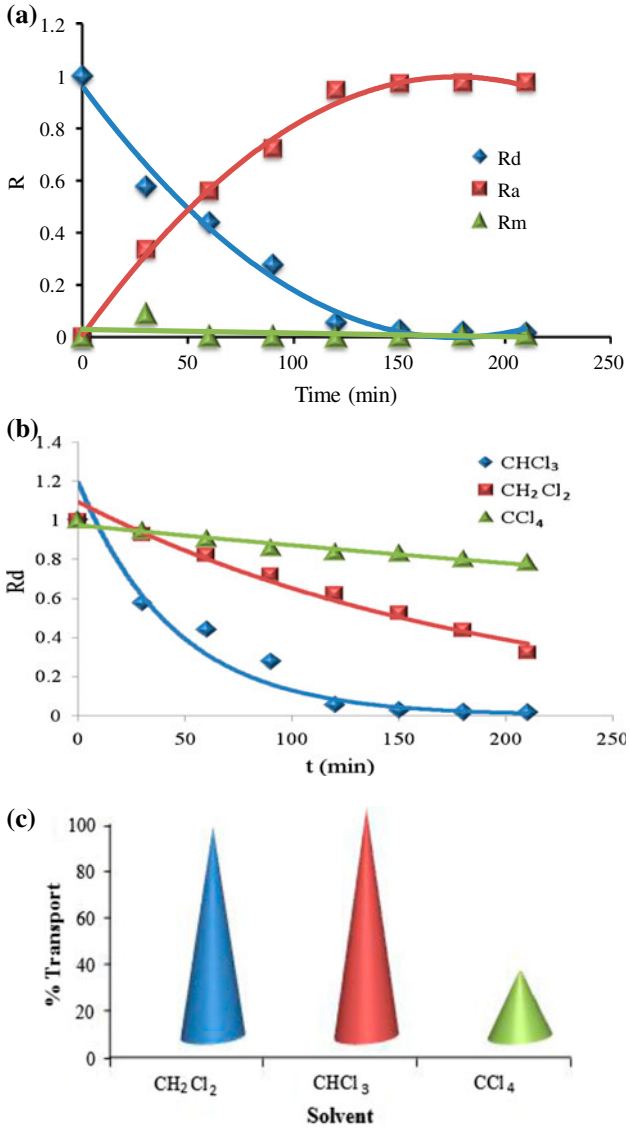

Fig. 5. (a) Time dependence of R_d, R_m, and R_a for the transport of MR membrane phase: 1×10^{-3} M carrier in chloroform, stirring rate 800 rpm at 298 K, (b) R_a variation versus time, and (c) % transportation for the transport of MR in different solvents.

analysis was carried out by non-linear curve fitting. Fig. 5(a) shows the variation of R_d, R_m, and R_a with time through BLM.

3.3.2. Effect of solvent

The stabilization of BLM is highly influenced by nature of the solvent. Moreover, solubility of the complex as well as penetration power of the dye in receiving phase is also dependent on the viscosity of the solvent. Therefore, the impacts of solvent on the transport efficiency and kinetic parameters were studied, while obtained results are collected in Table 1 and Fig. 5 (b) and (c). The data reveal that the maximum MR was transported in $CHCl_3$ and membrane entrance and exit rate constants increase in the order of $CCl_4 < CH_2Cl_2 < CHCl_3$. The high viscosity of CCl_4 relative to $CHCl_3$ can be the obvious explanation for low MR transport in CCl_4. In contrast, CH_2Cl_2 owing to high dipolar moment, high dielectric constant, and high miscibility in water is also not found appropriate for making stable BLM like $CHCl_3$ [12].

3.3.3. Effect of stirring speed

The dye transfer between two phases is highly affected by the variation of stirring speed. The experiments were carried out at varying stirring speeds of the membrane phase from 200, 400, 600, and 800 rpm at 298 K using 1×10^{-3} M of carrier **1** in $CHCl_3$. The results are compiled in Table 2 and Fig. 6(a). The maximum MR transport was observed at high stirring speed and it is also evident from the higher flux, k_1 and k_2 values. Conversely, the t_{max} values were lower at high stirring speed. The probable explanation for the maximum MR transport at high stirring speed is efficient mixing of donor and receiving phases which truly minimize the concentration polarization of MR in donor phase and accelerates its transport towards the receiving phase. In current study, the 98% of MR was transported to the receiving phase at 800 rpm (Fig. 6(b)).

3.3.4. Effect of concentration of carrier

Carrier being a leading phase transfer is the important component of BLM transport. It effectively transfers dye into the receiving phase after diffusing through the organic phase. The transport experiments

Table 1
Kinetic parameters of MR in different solvents

Solvent	$k_1 \times 10^2$ (min^{-1})	$k_2 \times 10^2$ (min^{-1})	R_m^{max}	t_{max} (min)	$J_d^{max} \times 10^2$ (min^{-1})	$J_a^{max} \times 10^2$ (min^{-1})	Dye transported (%)
CH_2Cl_2	0.8	3.0	0.067	90	−0.5	0.5	90
$CHCl_3$	2.2	8.1	0.088	30	−1.4	1.4	98
CCl_4	0.1	1.2	0.026	300	−0.1	0.1	29

Table 2
Kinetic parameters of MR at different stirring rates (solvent $CHCl_3$; T = 298 K)

Stirring rate (rpm)	$k_1 \times 10^2$ (min^{-1})	$k_2 \times 10^2$ (min^{-1})	R_m^{max}	t_{max} (min)	$J_d^{max} \times 10^2$ (min^{-1})	$J_a^{max} \times 10^2$ (min^{-1})	Dye transported (%)
200	0.4	1.9	0.056	150	−0.3	0.3	67
400	1.2	2.3	0.065	120	−0.6	0.6	87
600	1.6	2.8	0.077	90	−0.8	0.8	91
800	2.2	8.1	0.088	30	−1.4	1.4	98

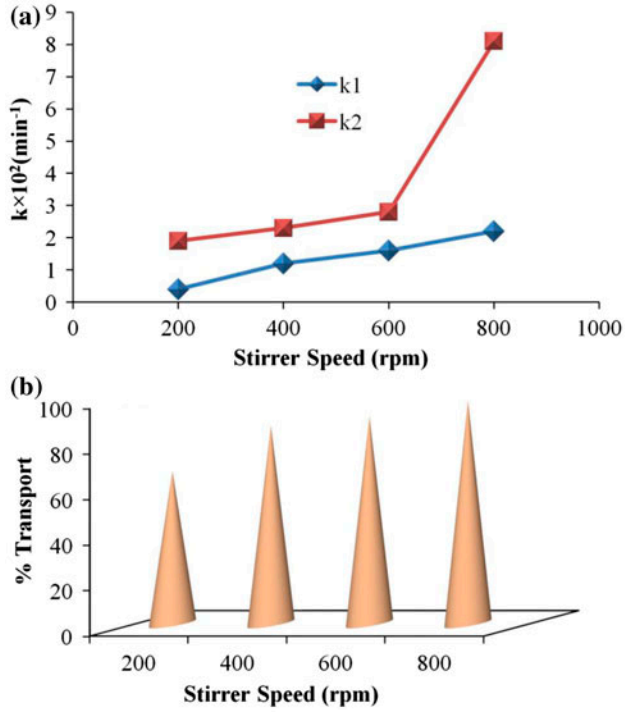

Fig. 6. Effect of stirring rate on (a) flux values, and (b) % transportation of MR through BLM.

were conducted by diluting the stock solution of carrier **1** from 1×10^{-3} to 1×10^{-5} M in $CHCl_3$. The different concentrations were used in BLM at 298 K and 800 rpm. The results are presented in Table 3 and Fig. 7(a)–(c). It can be seen from results that the flux values for MR are increased with rise in the carrier concentration. The dependence of flux values on concentration is supported from Eqs. (6) and (7) as well. At low carrier concentration, the interface between donor and receiving phase is not fully saturated with carrier and hence MR transport is low. The opposite trend is true for the high carrier concentration. Furthermore, blank experiment was also performed without carrier to examine the role of solvent in the MR transport. Since any appreciable movement of MR was not observed across BLM in blank experiment, therefore, the MR transport is fully assumed to be dependent on the carrier **1**.

3.4. Lifetime of the BLM

The reproducibility of the MR transport under optimum conditions was checked for multiple cycles through developed BLM system. The % transport of the MR after 120 min using five replicates of BLM solution was found to be 98% ± 1%.

3.5. Uphill transport mechanism

The phenomenon regarding transport mechanism is illustrated in Fig. 8(a). The MR transport from the donor phase towards the receiving phase by crossing organic phase containing carrier **1** is accomplished under following steps.

(1) The diffusion of MR from donor to membrane interface via aqueous boundary layer by making complexation with carrier **1**.

Table 3
Effect of carrier **1** concentration on the kinetic parameters for the transport of MR. (solvent: $CHCl_3$; 298 K and 800 rpm)

Conc.	$k_1 \times 10^2$ (min^{-1})	$k_2 \times 10^2$ (min^{-1})	R_m^{max}	t_{max} (min)	$J_d^{max} \times 10^2$ (min^{-1})	$J_a^{max} \times 10^2$ (min^{-1})	Dye transported (%)
1×10^{-5}	0.6	1.5	0.059	180	−0.3	0.3	66
1×10^{-4}	1.2	1.7	0.074	150	−0.5	0.5	87
1×10^{-3}	2.2	8.1	0.088	30	−1.4	1.4	98

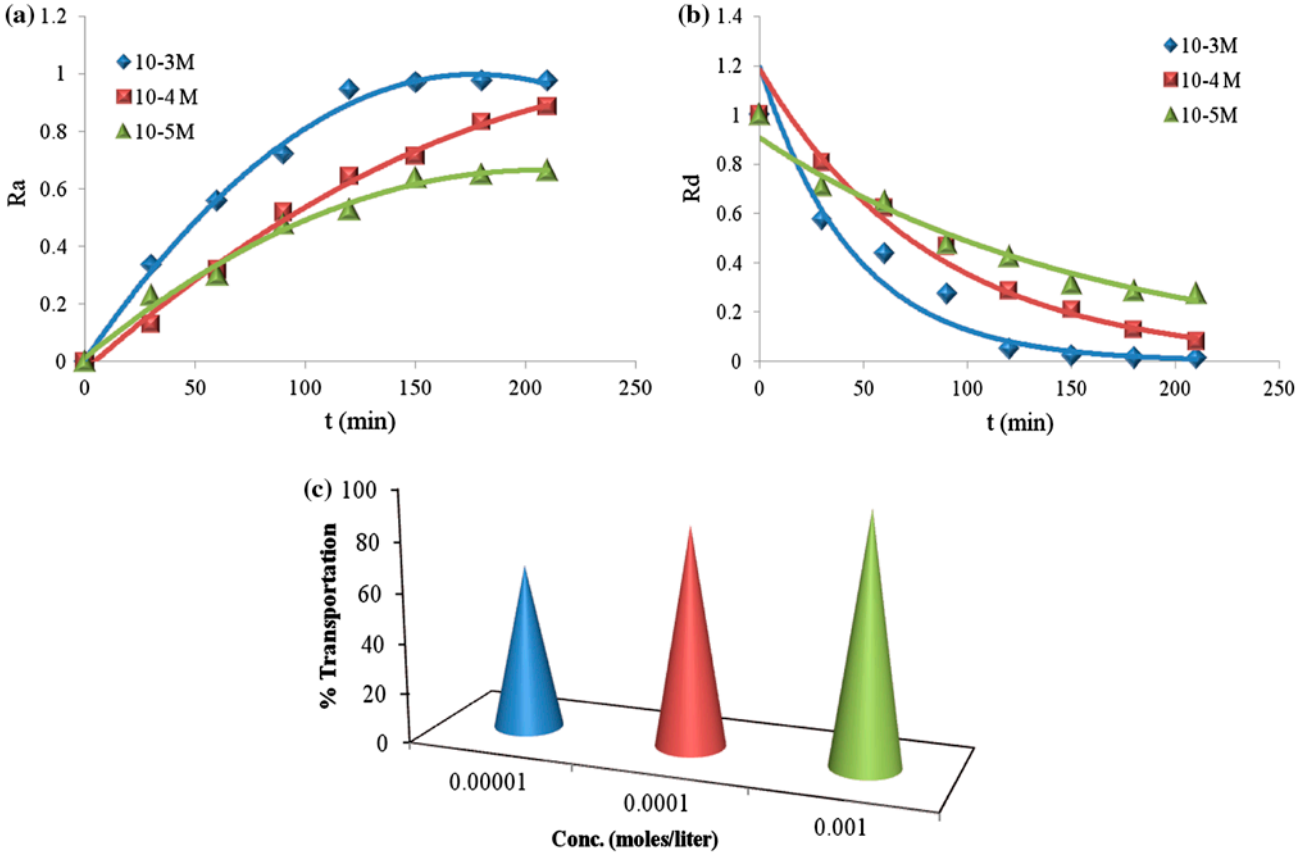

Fig. 7. Time variation of reduced concentration (a) R_a, (b) R_d and (c) % transportation of MR transported through BLM at different carrier concentration in CH_2Cl_2.

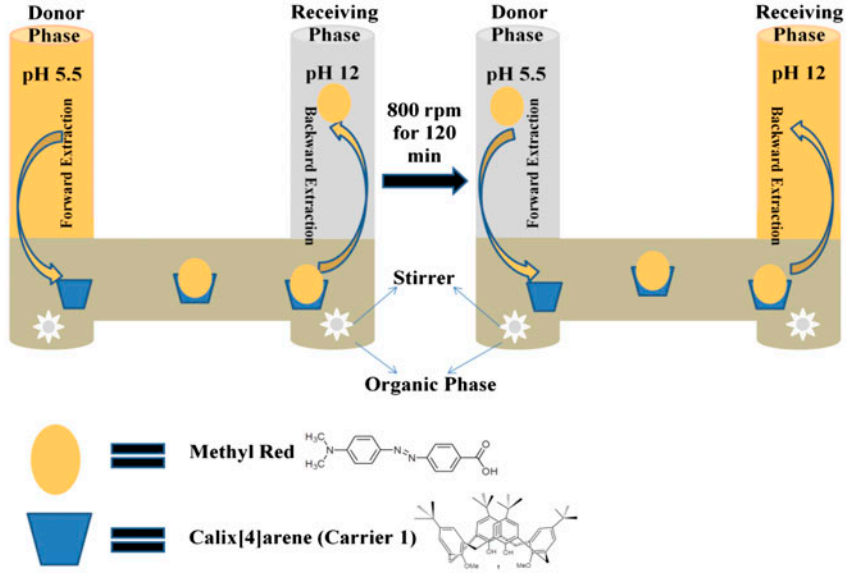

Fig. 8. (a) Transport mechanism of MR from donor to receiving phase through BLM using carrier **1**, and (b) Proposed interaction/complexation between MR and carrier **1**.

Table 4
Transport of MR in real and experimental samples through BLM

Sample	Remained (%)	Transported (%)
MR	2	98
Real sample	0.6	99.4

(2) The complex thus formed moves through the membrane towards the receiving phase due to the potential gradient developed between donor and receiving phase.
(3) At the junction between membrane and acceptor phase decomplexation of the **1**-MR takes place due to alkaline pH of the receiving phase where both MR and the carrier **1** lose their protons and results in the successive and efficient release of MR into the receiving phase.
(4) Finally, the carrier is free of MR and diffuses back into the organic membrane to carry another MR molecule and the cycle continues till 98% transfer of MR successfully takes place.

Consequently, the whole process is governed with continuous stirring of the system under optimum conditions.

3.6. Application to real wastewater samples

The applicability of the developed BLM method was tested by real wastewater sample that was collected from the locality of Jamshoro industrial area. The sample was analyzed by UV–visible spectrophotometer to check the absorbance before its transport through BLM. Consequently, under optimized conditions, 10 mL of this sample solution was taken as donor phase and transferred to receiving phase through BLM using carrier **1**. The results are elaborated in Table 4, which shows that carrier **1** can effectively transport a dye mixture containing MR from real sample. Furthermore, Fig. 9 provides a clear justification regarding the efficiency of carrier **1** that is conveniently transporting dyes with absorption maximum in the range of ≈330 – ≈520 nm from the industrial wastewater.

3.7. Comparative study

BLM technique can be compared in its efficiency as well as simplicity with other recently published conventional and non-conventional techniques for the remediation of dyes such as electrochemical degradation [28], liquid–liquid extraction [29] biodegradation [30], oxidation [31], and adsorption [4]. Electrochemical degradation process can certainly be adapted for the remediation of dyes but formation of hydroxide sludge is major drawback. Biodegradation is another alternative method but due to complex aromatic structure and molecular size it shows very low degradability for dyes and pigments. Oxidation process is another remarkable technique to eliminate the noxious pollutants however, oxidation works only at lower concentrations. Besides this, adsorption plays a vital role at higher concentrations but regeneration of most

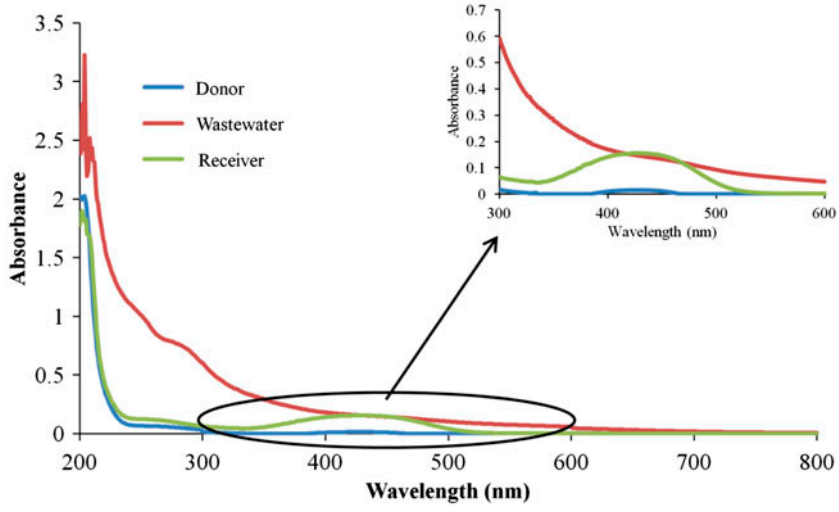

Fig. 9. Absorption spectra of wastewater. An inset showing confined region of MR absorption.

Table 5
Comparative study of BLM with other techniques for different dyes

Technique	Active specie	Dye	Drawbacks	Time taken for the removal (min)	Energy consumption	Tediousness	% Removal (%)	Ref.
Electrochemical degradation	Electrochemical reactor	Remazol Black B	Formation of hydroxide sludge	180	Less	High	~90	[28]
Ionic liquid-based dispersive liquid–liquid extraction	Binary solution of extraction and disperser solvent	Congo red	Expensive and uneconomical method for industries	<7	Medium	Less	>95	[29]
Biodegradation	Pseudomonas aeruginosa BCH	Acid violet 19	Low degradability due to complex structure	30	Medium	Medium	98	[30]
Oxidation	Homogeneous and heterogeneous catalysts	Reactive yellow 81	Works only at lower concentrations	120	Medium	Medium	62.8	[31]
Adsorption	Calix[n]arene derivatives	Azo dyes	Regeneration of adsorbents are time consuming and expensive	60	Less	Medium	~96	[4]
BLM	Calix[4]arene derivative	MR	Needs technical improvements for commercial application	120	Less	Least	>98	This work

of the adsorbents is difficult except for activated carbon, but adsorption through activated carbon is expensive [32]. The data are summarized in Table 5, which reveals that in contrast to other techniques BLM is a versatile technique that can be frequently applied for the removal of dye with less energy consumption and high efficiency. Furthermore, Yang et al. [26,33] have recently reported that using four different calix[4]arene derivatives, 88% and 95% removal of dyes can be achieved which is higher than simple calix[4,6,8]arene [34]. The authors also claimed that the additional effect is due to the specific functionalities attached with the calix[4]arene. In contrast, the highest efficiency of present study can also be justified on the basis of functionality attached on the calix[4] arene skeleton. Moreover, carrier **1** can also be compared for its efficiency with previously reported calixarenes and their derivatives [26,33] in BLM due to having ability to remove MR >98% within 120 min.

4. Conclusion

The study reveals the efficiency of calix[4]arene derivative (**1**) as an excellent carrier for the dyes, especially MR from the donor phase to receiving phase through BLM. The complexation phenomenon was studied using Job's plot which suggested 1:1 complexation between host and guest molecules. The apparent rate constants (k_1 and k_2) for interfacial MR transport have found to be dependent on various parameters such as pH, stirrer speed, carrier concentration, and solvent. Experiments show that the solvent and carrier can be efficiently reused for multiple cycles, which justifies the economical feasibility of the process as compared to other separation techniques. The proposed method was applied to industrial wastewater and found to be 99% efficient for the transport of dyes. This study provides the promising platform for the treatment of wastewater containing different dyes as contaminant.

Acknowledgments

We would like to thank Higher Education Commission Islamabad (No. 2Ps1-324) and the National Centre of Excellence in Analytical Chemistry, University of Sindh, Jamshoro for the financial assistance.

References

[1] M.A. Mahmoud, A. Poncheri, Y. Badr, M.G. Abd, El. Wahed, Photocatalytic degradation of methyl red dye, South Afr. J. Sci. 105 (2009) 299–303.
[2] Student Safety Sheets, Dyes & Indicators ©CLEAPSS 2007.
[3] G.M. Nisola, E. Cho, A.B. Beltran, M. Han, Y. Kim, W.J. Chung, Dye/water separation through supported liquid membrane extraction, Chemosphere 80 (2010) 894–900.
[4] E.Y. Ozmen, S. Erdemir, M. Yilmaz, M. Bahadir, Removal of carcinogenic direct azo dyes from aqueous solutions using calix[n]arene derivatives, Clean—Soil Air Water 35 (2007) 612–616.
[5] W.J. Lau, A.F. Ismail, Polymeric nanofiltration membranes for textile dye wastewater treatment: Preparation, performance evaluation, transport modelling, and fouling control—A review, Desalination 245 (2009) 321–348.
[6] A. Razaee, M.T. Ghaneian, S.J. Haashemian, G.H. Moussavi, G.H. Ghanizedeh, E. Hajizadeh, Photochemical oxidation of reactive blue-19 Dye (RB-19) in textile wastewater by UV/$K_2S_2O_8$ process, Iran J. Environ. Health Sci. Eng. 5 (2008) 95–100.
[7] S.S. Madaeni, Z. Jamali, N. Islami, Highly efficient and selective transport of methylene blue through a bulk liquid membrane containing Cyanex 301 as carrier, Sep. Purif. Tech. 81 (2011) 116–123.
[8] M. Ersoz, Transport of mercury through liquid membranes containing calixarene carriers, Adv. Colloid Interface Sci. 134–135 (2007) 96–104.
[9] M. Kermiche, S. Djerad, Facilitated transport of copper through bulk liquid membrane containing di-2ethylhexyl phosphoric acid, Desalin. Water Treat. 36 (2011) 261–269.
[10] I. Zaharia, I. Diaconu, E. Ruse, G. Nechifor, The transport of 3-aminophenol through bulk liquid membrane in the presence of aliquat 336 Digest, J. Nanomat. Biostructures 7 (2012) 1303–1314.
[11] I. Zaharia, I. Diaconu, G. Nechifor, The pH role in the transport of active principles of drugs through agitated bulk liquid membrane, U.P.B. Sci. Bull. Series B 74 (2012) 61–70.
[12] R. Tandlich, Application of liquid membranes in wastewater treatment, in: V.S. Kislik (Ed.), Liquid Membranes Principles and Applications in Chemical Separations and Wastewater Treatment, Elsevier B.V, 2010, pp. 357–400 (Chapter 8).
[13] G. Muthuraman, M. Ibrahim, Use of bulk liquid membrane for the removal of Cibacron Red FN-R from aqueous solution using TBAB as a carrier, J. Indus. Eng. Chem. 19 (2012) 444–449.
[14] N. Hajarabeevi, I.M. Bilal, D. Easwaramoorthy, K. Palanivelu, Facilitated transport of cationic dyes through a supported liquid membrane with D_2EHPA as carrier, Desalination 245 (2009) 19–27.
[15] G. Muthuraman, K. Palanivelu, Transport of textile cationic dyes using cationic carrier by bulk liquid membrane, J. Sci. Ind. Res. 64 (2005) 529–533.
[16] G. Muthuraman, K. Palanivelu, Transport of textile dye in vegetable oils based supported liquid membrane, Dyes Pigm. 70 (2006) 99–104.
[17] C. Das, M. Rungta, G. Arya, S. DasGupta, S. De, Removal of dyes and their mixtures from aqueous solution using liquid emulsion membrane, J. Hazard. Mater. 159 (2008) 365–371.
[18] A.D. Stancu, M. Hillebrand, C. Tablet, L. Mutihac, β-Cyclodextrin derivative as chiral carrier in membrane transport of some aromatic amino acids, J. Incl. Phenom. Macrocycl. Chem. 78 (2014) 71–76.
[19] F.N. Memon, S. Memon, Calixarenes: A versatile source for the recovery of reactive blue-19 dye from industrial wastewater, Pak. J. Anal. Environ. Chem. 13 (2012) 62–72.
[20] F.N. Memon, S. Memon, Differential recognition of D and L-alanine by calix[4]arene amino derivative, J. Incl. Phenom. Macrocycl. Chem. 77 (2013) 413–420.
[21] F.T. Minhas, S. Memon, I. Qureshi, M. Mujahid, M.I. Bhanger, Facilitated kinetic transport of Cu(II) through a supported liquid membrane with calix[4]arene as a carrrier, C. R. Chimie 16 (2013) 742–751.
[22] F.N. Memon, S. Memon, F.T. Minhas, Rapid transfer of methyl red using calix[6]arene as a carrier in a bulk liquid membrane, C. R. Chimie 17 (2014) 577–585.
[23] I.H. Gubbuk, O. Gungor, Transport of methylene blue through bulk liquid membrane containing calix[8] arene derivative, Desalin. Water Treat. 52 (2014) 5575–5582.
[24] S. Memon, M. Yilmaz, Synthesis and complexation studies of 1,3—Dialkylated p-*tert*-butylcalix[4]arene telomers, React. Funct. Polym. 44 (2000) 227.
[25] C.J. Pedersen, Ionic complexes of macrocyclic polyethres, Fed. Proc. 27 (1968) 1305–1309.
[26] F. Yang, W. Liu, J. Xie, X. Bai, H. Guo, Novel deep-cavity calix[4]arene derivatives with large s-triazine conjugate systems: Synthesis and complexation for dyes, J. Incl. Phenom. Macrocycl. Chem. 76 (2013) 311–316.
[27] G. Muthuraman, K. Palanivelu, T.T. Teng, Transport of cationic dye by supported liquid membrane using D_2EHPA as the carrier, Color. Technol. 126 (2010) 97–102.
[28] P.A. Soloman, C.A. Basha, M. Velan, V. Ramamurthi, K. Koteeswaran, N. Balasubramanian, Electrochemical degradation of remazol black b dye effluent, Clean—Soil Air Water 37 (2009) 889–900.
[29] M. Gharehbaghi, F. Shemirani, A novel method for dye removal: Ionic liquid-based dispersive liquid–liquid extraction (IL-DLLE), Clean—Soil Air Water 40 (2012) 290–297.
[30] S.B. Jadhav, S.M. Yedurkar, S.S. Phugare, J.P. Jadhav, Biodegradation studies on acid violet 19, a triphenylmethane dye, by pseudomonas aeruginosa BCH, Clean—Soil Air Water 40 (2012) 551–558.
[31] Z. Eren, Degradation of an azo dye with homogeneous and heterogeneous catalysts by sonophotolysis, Clean—Soil Air Water 40 (2012) 1284–1289.

[32] J.W. Lee, S.P. Choi, R. Thiruvenkatachari, W.G. Shim, H. Moon, Evaluation of the performance of adsorption and coagulation processes for the maximum removal of reactive dyes, Dyes Pigm. 69 (2006) 196–203.
[33] F. Yang, Y. Zhang, H. Guo, X. Wei, Highly efficient liquid membrane transport of dyes using calix[4] arene-linked triphenylene dimers as carriers, Sep. Sci. Tech. 48 (2013) 1565–1571.
[34] O. Gungor, A. Yilmaz, S. Memon, M. Yilmaz, Evaluation of the performance of calix[8]arene derivatives as liquid phase extraction material for the removal of azo dyes, J. Hazard. Mater. 158 (2008) 202–207.